International Journal of Quantum Information
Vol. 3, No. 3 (2005) 441–462

World Scientific
www.worldscientific.com

STABILITY OF THE QUANTUM FOURIER TRANSFORMATION ON THE ISING QUANTUM COMPUTER

GIUSEPPE LUCA CELARDO
Dipartimento di Matematica e Fisica, Università Cattolica,
via Musei 41, 25121 Brescia, Italy
celardo@dmf.bs.unicatt.it

CARLOS PINEDA
Universidad Nacional Autónoma de México,
Apdo. Postal 20-364, Mexico D. F. 01000, Mexico
carlospgmat03@yahoo.com

MARKO ŽNIDARIČ
Physics Department, Faculty of Mathematics and Physics,
University of Ljubljana, Slovenia
znidaricm@fiz.uni-lj.si

Received 16 November 2004

We analyze the influence of errors on the implementation of the quantum Fourier transformation. Two kinds of errors are studied: (i) systematic errors due to off-resonant transitions and (ii) errors due to an external perturbation. The scaling of errors with system parameters and the number of qubits is analyzed. To suppress off-resonant transitions, we use correcting pulses while in order to suppress errors due to an external perturbation, we use an improved quantum Fourier transformation algorithm. As a result, the fidelity of quantum computation is increased by several orders of magnitude and is thus stable in a much wider range of physical parameters.

Keywords: Ising; quantum computation; quantum Fourier transform; decoherence; fidelity.

PACS Number(s): 03.67.Lx, 03.67.Pp, 75.10.Pq

1. Introduction

Quantum information theory[1] is a rapidly evolving field. It uses quantum systems to process information thereby achieving things not possible with classical resources alone. Quantum secure communication for instance is already commercially available. Quantum computation on the other hand is still far from being useful. Two serious obstacles to overcome in building a large quantum computer are: (i) one must be able to control the evolution in order to precisely implement quantum gates, and (ii) one must suppress external influences. Errors in both cases are caused by the

perturbation of an ideal quantum computer, either by internal imperfections or by coupling to the "environment." In the present paper, we study both kind of errors, in particular their scaling with the number of qubits, in order to envisage the obstacles and demands of building a large quantum computer. We also suggest possible ways to minimize these errors.

We choose a concrete model of a quantum computer and a concrete algorithm. As one of the main things we want to study is the scaling of errors with the size of the computer, we do not limit ourselves to any of the existing experimentally realizable models because their success for a large number of qubits is far from guaranteed. Rather we choose a simple abstract Ising quantum computer model (IQC),[2] having all the essential properties of a future quantum computer: (i) it is a universal quantum computer, (ii) it is scalable with the number of qubits, and (iii) it is one of the simplest models having the first two properties. Multi-qubit gates are possible through inter-qubit coupling; in fact, we choose the simplest possible one, namely nearest-neighbor coupling. The pulses by which we perform quantum gates are not ideal, thereby causing off-resonant transitions. Such unwanted transitions are expected to be a generic feature of any experimental implementation of a quantum computer. In adition, we also study the influence of external perturbations on the algorithm stability. All these we feel, will be the necessary ingredents of any large quantum computer, and we believe our results have relevance beyond the specifics of the IQC model.

For the quantum algorithm we will discuss the quantum Fourier transformation (QFT). The first reason to choose the QFT is that it is one of the most useful quantum algorithms, giving an exponential speedup over the best classical procedure known. Furthermore, it is also one of the ingredients of some other important algorithms, e.g. Shor's factoring algorithm.[3] The second reason is that the QFT is a complex algorithm, where by complex we mean it has more than $\mathcal{O}(n)$ number of quantum gates as opposed to previously studied more simple algorithms, where the number of gates scales only linearly with the size of the computer (e.g. the entanglement protocol[4]). It is easy to imagine that in most useful quantum algorithms, the size of the program will grow faster than linearly with the number of qubits n and therefore it is important to see how errors accumulate in such algorithms. This importance is confirmed by our results showing that errors due to unwanted transitions for the QFT grow as the *square* of the number of pulses and not *linearly* as in algorithms with a linear $\mathcal{O}(n)$ number of gates, for a typical initial state.

For the QFT algorithm running on the IQC, we analyze errors due to spurious transitions caused by pulses (these we call *intrinsic errors*), and errors due to the coupling with an external "environment" (called *external errors*), modeled by a random Hermitian matrix from a Gaussian unitary ensemble (GUE).[7] We minimize intrinsic errors by applying some additional pulses to correct most probable errors[6] and by doing this, we are able to suppress intrinsic errors by several orders of magnitude. To suppress external errors due to a GUE perturbation, we use a previously proposed improved quantum Fourier transformation (IQFT),[8] which is more stable against GUE perturbations in a certain range of parameters. We analyze in detail

the dependence of errors on all relevant parameters. With this analysis, we can set the limits between which parameters of the IQC should lay in order to preserve the stability of computation and how this demands change with the size of the quantum computer. In our approach to decrease errors, we do not use error correcting codes for the following reasons: we want to remove as many errors as we can at the lowest possible level and second, the intrinsic and particularly multi-qubit external errors are not easily handled by the error correcting codes (see Ref. 10 and references therein).

The outline of the paper is as follows. In Sec. 2, we repeat the definition of the IQC and in Sec. 3, we summarize the linear response formalism, which is the main theoretical tool for studying fidelity. In Sec. 4, we study intrinsic and external errors, first separately and then simultaneously. In the appendix, we present the pulse sequences used to implement the QFT and the IQFT algorithms.

2. The Ising Quantum Computer

The IQC consists of a one-dimensional chain of n equally spaced identical spin 1/2 particles coupled by a nearest neighbor Ising interaction of strength J, such that parallel spins are favored over anti-parallel ones by an energy difference of J (we set $\hbar = 1$ throughout the paper). The quantum computer is operated via an external magnetic field having two components. The first one is a permanent magnetic field oriented in the z-direction with a constant gradient which allows the selective excitation of individual spins, while the second one is a sequence of T circular polarized fields in the x-y plane (which are called pulses), with different frequencies $\nu^{(m)}$, amplitudes (proportional to the Rabi frequencies $\Omega^{(m)}$), phases $\varphi^{(m)}$ and durations $\tau^{(m)}$ for the mth pulse, in which the protocol is encoded. A particular orientation of the register allows one to suppress the dipole–dipole interaction between spins.[11,12]

The Hamiltonian of the system is

$$H = -\frac{1}{2}\sum_{l=0}^{n-1}\omega_l\sigma_l^z - \frac{J}{2}\sum_{l=0}^{n-2}\sigma_l^z\sigma_{l+1}^z - \sum_{m=1}^{T}V^{(m)}(t)\Theta^{(m)}(t) \tag{1}$$

with

$$V^{(m)}(t) = \frac{\Omega^{(m)}}{4}\sum_{l=0}^{n-1}(\sigma_l^- \exp\{-\mathrm{i}(\nu^{(m)}t + \varphi^{(m)})\} + \text{h.c.}), \tag{2}$$

where $\Theta^{(m)}(t)$ is equal to one during the mth pulse and zero otherwise, $\sigma_l^{x,y,z}$ are the usual Pauli operators for lth spin and $\sigma_l^{\pm} = \sigma_l^x \pm \mathrm{i}\sigma_l^y$. Due to the constant gradient of the permanent magnetic field, the Larmor frequencies depend linearly on l, $\omega_l = (l+1)a$. By appropriately choosing the energy units, we fix $J = 1$ so the only relevant energy scales are $\Omega^{(m)}$ and a. The basis states are chosen such that $\sigma_l^z|0\rangle_l = |0\rangle_l$.

We shall introduce the following notation. Let P_i^{ac} indicate a pulse with frequency ν_i^{ac} resonant with the ith spin when its neighbors are in states "a" and "c".

This will induce the resonant transition $|\cdots a_{i+1}b_ic_{i-1}\cdots\rangle \to |\cdots a_{i+1}\bar{b}_ic_{i-1}\cdots\rangle$, named T_i^{ac}, if the pulse is a π pulse ($a, b, c \in \{0, 1\}$). Note that for edge qubits, i.e. $i \in \{0, n-1\}$, only one superscript is needed.

Operating the IQC in the *selective excitation regime*, i.e. $\Omega^{(m)} \ll J \ll a$, allows one to separate transitions induced by pulses into three sets: *resonant*, *near-resonant* and *non-resonant* according to the detuning Δ of the transition, which is the difference between the frequency of the pulse and the energy difference of the states involved in the transition. If Δ is exactly equal to zero, the transition is called resonant (T_i^{ac} induced by the pulse P_i^{ac}); if Δ is of the order of J, it is called near-resonant ($T_i^{a'c'}$ induced by the pulse P_i^{ac} with $\{a', c'\} \neq \{a, c\}$); if Δ is of the order of a, it is called non-resonant transition ($T_{i'}^{a'c'}$ induced by the pulse P_i^{ac} with $i' \neq i$). In the implementation of a protocol, resonant transitions are the ones wanted, while near-resonant and non-resonant transitions are a source of error.

In the two-level approximation,[11] a given unwanted transition with detuning Δ is induced with probability

$$p = \frac{\Omega^2}{\Omega^2 + \Delta^2} \sin^2\left(\rho \frac{\pi}{2} \sqrt{1 + \frac{\Delta^2}{\Omega^2}}\right), \tag{3}$$

where ρ is the dimensionless duration of the pulse (e.g. for a π pulse $\rho = 1$ and for $\pi/2$ pulse it is $1/2$). The most probable unwanted transitions are the near-resonant ones and these can be suppressed by a generalized $2\pi k$ method as briefly described in the next paragraph.

For $P_i^{10} (= P_i^{01})$ pulses, all near-resonant transitions have the same detuning Δ and the transition probability p will be zero, provided we set the Rabi frequency to

$$\Omega = \frac{\Delta}{\sqrt{4k^2 - 1}}, \tag{4}$$

with k an integer. Since for near-resonant transitions $\Delta = \mathcal{O}(J)$, for all pulses the Rabi frequency is of the order of J/k. On the other hand, for P_i^{00} and P_i^{11} pulses the near-resonant transitions have two different detunings. Therefore, it is impossible to suppress both transitions with a single pulse. This problem can be overcome adding an additional correcting P_i^{10} pulse. The combination of these pulses in order to suppress all near-resonant transitions is called a Q-pulse, denoted by $Q_{i\rho}^{ac}$ when doing a $\rho\pi$ rotation of the ith qubit if neighbors are in states "a" and "c". This method to eliminate all near-resonant transitions is called the generalized $2\pi k$ method and is the best known procedure to induce transitions on the IQC. We refer the interested reader to Ref. 6 for further details. A previous study of Shor's algorithm on the IQC[5] did not use this method. Q-pulses are the basic building blocks of gates, which in turn are the building blocks of algorithms such as the QFT and the IQFT.

The QFT for $n = 4$ qubits can be written as

$$\mathrm{U_{QFT}} = \mathrm{TA_0B_{01}B_{02}B_{03}A_1B_{12}B_{13}A_2B_{23}A_3}. \tag{5}$$

There are in total n Hadamard gates (A_j), $n(n-1)/2$ two-qubit B gates, $\mathrm{B}_{jk} = \mathrm{diag}\{1,1,1,\exp(i\theta_{jk})\}$ with $\theta_{jk} = \pi/2^{k-j}$, and one transposition gate T which reverses the order of qubits (e.g. $\mathrm{T}|001\rangle = |100\rangle$). In total, there are $n(n+1)/2+1$ gates. The IQFT algorithm,[8] which is more stable in the presence of GUE perturbations, for $n = 4$ qubits is

$$\begin{aligned} U_{\mathrm{IQFT}} = {} & \mathrm{TA}_0\mathrm{R}_{01}\mathrm{R}_{02}\mathrm{R}_{03}\mathrm{G}_{01}\mathrm{G}_{02}\mathrm{G}_{03} \\ & \times \mathrm{A}_1\mathrm{R}_{12}\mathrm{R}_{13}\mathrm{G}_{12}\mathrm{G}_{13}\mathrm{A}_2\mathrm{R}_{23}\mathrm{G}_{23}\mathrm{A}_3, \end{aligned} \tag{6}$$

where $\mathrm{G}_{ij} := \mathrm{R}_{ij}^{\dagger}\mathrm{B}_{ij}$. The R gate is defined by $\mathrm{R}_{ij}|\cdots a_i \cdots b_j \cdots\rangle := (-1)^{b_j}|\cdots a_i \cdots (\overline{a_i} \oplus b_j)\cdots\rangle$. In total, there are n^2+1 gates in the IQFT, i.e. roughly two times as many as for the QFT.

Each gate for the QFT or the IQFT [Eqs. (5) and (6)] must in turn be implemented by several pulses (see appendix). The number of pulses for the QFT grows as $\sim 18n^3$ whereas it grows as $\sim 54n^3$ for the IQFT. This number can become very large, e.g. for the IQFT and $n = 10$ one has 44,541 pulses.

Note that the implementation of quantum gates on the IQC is easier in the interaction picture since one can ignore large phases arising from the free evolution. Here the interaction picture is defined by the transformation $\psi_{\mathrm{int}} = \exp(iH_0t)\psi_{\mathrm{sch}}$, where H_0 is time-independent part of the Hamiltonian H (1) and ψ_{sch} is the usual solution of time-dependent Schrödinger equation with the full Hamiltonian H, i.e. the Schrödinger picture.[a] Therefore, pulse sequences used in the paper implement the intended gates in the interaction picture.

Throughout the paper, our basic unit of time will be either a gate [as written for instance in Eqs. (5) and (6)] or a pulse. A single exception will be the paragraph discussing the correlation function of intrinsic errors, where the basic unit is a Q-pulse, which is composed of one or two pulses. The reason is that Q-pulses are the smallest unit of time, for which near-resonant transitions can be completely suppressed.

3. Linear Response Theory

As a criterion for stability, we shall use the fidelity $F(t)$, defined as an overlap between a state $\psi(t)$ obtained by the evolution with an ideal algorithm and $\psi_\delta(t)$ obtained by the perturbed evolution:

$$F(t) = |\langle\psi_\delta(t)|\psi(t)\rangle|^2, \tag{7}$$

where $|\psi(t)\rangle = U(t)|\psi(0)\rangle$ and $|\psi_\delta(t)\rangle = U^\delta(t)|\psi(0)\rangle$. To simplify matters, we shall assume time t to be a discrete integer variable, denoting some basic time unit of an algorithm. The quantity measuring the success of the whole algorithm is the fidelity $F(t)$ at $t = T$, where T denotes the total time. One of the most useful approaches to

[a] Even when we add an external perturbation to the Hamiltonian, we will refer to the interaction picture as the one defined here.

studying fidelity is using the linear response formalism in terms of the correlation function of the perturbation; for a review see Ref. 13. This approach has several advantages. First, it rewrites the complicated quantity fidelity in terms of a simpler one, namely the correlation function, simplifying the understanding of the fidelity. Second, the scaling of errors with the perturbation strength, Planck's constant and with the number of qubits is easily deduced. Furthermore, as in practice one is usually interested in the regime of high fidelity, linear response is typically enough.

First, we shall shortly repeat linear response formulas as they will be useful for our discussion later. Let us write an ideal algorithm up to time t as $U(t)$:

$$U(t) = U_t U_{t-1} \cdots U_1, \tag{8}$$

where U_i is the ith gate (pulse). If $t = T$, we have a decomposition of the whole algorithm.

The perturbed algorithm can be similarly decomposed into gates

$$U^\delta(t) = U_t^\delta U_{t-1}^\delta \cdots U_1^\delta. \tag{9}$$

Each perturbed gate U_j^δ is now written as

$$U_j^\delta = \exp(-\mathrm{i}\delta V_j) U_j, \tag{10}$$

where V_j is the perturbation of jth gate and δ is a dimensionless perturbation strength. For any perturbed gate, one can find a perturbation generator V, such that relation (10) holds. Observe that the distinction between the perturbation strength δ and the perturbation generator V in Eq. (10) is arbitrary. If one is given an ideal gate U and a perturbed one U^δ, one is able to calculate only the product δV. This arbitrariness can always be fixed by demanding for instance that the second moment of the perturbation V in a given state is equal to one.

To lowest order in δ, fidelity can be written as[9]

$$F(t) = 1 - \delta^2 \sum_{t_1,t_2=1}^{t} C(t_1, t_2), \tag{11}$$

where the correlation function of the perturbation is

$$C(t_1, t_2) = \langle V_{t_1}(t_1) V_{t_2}(t_2) \rangle - \langle V_{t_1}(t_1) \rangle \langle V_{t_2}(t_2) \rangle \tag{12}$$

with $V_j(t) = U^\dagger(t) V_j U(t)$ being the perturbation of jth gate propagated by an ideal algorithm up to time t. The brackets $\langle \cdot \rangle$ denote the expectation value in the initial state. Throughout the paper, we average over an ensemble of random Gaussian initial states to reduce statistical fluctuations. Note that the time dependence of the correlation function (12) is due to two reasons: one is time dependence due to the propagation with the unperturbed Hamiltonian (time index in brackets) and the second one is due to the time dependence of the perturbation itself (time index as a subscript) since one can have different perturbations at different times. Expression (11) is the main result of the linear response theory of fidelity. From this, one can see that decreasing the correlation sum (or even making it zero, see Ref. 14)

will increase the fidelity. In Ref. 8, stability of the QFT algorithm was considered with respect to static GUE perturbation. Analyzing the correlation function, the authors were able to design an improved QFT algorithm (IQFT) which increases fidelity.

We are mainly interested in the fidelity $F(T)$ at the end of an algorithm. The final time T in efficient quantum algorithms depends on the number of qubits in a polynomial way, say as $T \propto n^p$. The power p depends on the algorithm considered and of course also on our decomposition of the algorithm into gates (pulses). For the QFT and the IQFT algorithms with decomposition into gates, Eqs. (5) and (6), one has $p = 2$. On the other hand, for the implementation of the QFT on the IQC one needs $T \propto n^3$ ($p = 3$) basic electromagnetic pulses, as one is not able to directly perform B_{jk} gates on distant qubits but has to instead use a number of pulses proportional to the distance between the qubits $|j - k|$. If the correlation function decays sufficiently fast, the fidelity will decay like $1 - F \propto \delta^2 n^p$ whereas in the case of slow correlation decay, the fidelity will decay as $1 - F \propto \delta^2 n^{2p}$. In the extreme case of perturbations at different times being statistically uncorrelated (very fast decay of correlations) $\langle V_j V_k \rangle \propto \delta_{jk}$, one can go beyond the perturbation theory and obtains the exact formula $F = \exp(-\delta^2 T)$.[8] Therefore, in the limit of a large quantum computer (large n) strongly correlated static errors (implying slow decay of correlations) will be dominant. When discussing errors caused by the coupling to the environment, we shall focus on static perturbations, meaning the same perturbation on all gates, $V_k = V_j = V$, as this component will dominate the large n behavior.

4. Errors in the Quantum Fourier Transformation

Errors in an experimental implementation of the QFT algorithm on the IQC can be of three kinds: (i) due to unwanted transitions caused by electromagnetic pulses, (ii) due to the coupling with external degrees of freedom, and (iii) due to the variation of system parameters in the course of algorithm execution. In the present paper, we shall discuss only the first two errors. Errors due to electromagnetic pulses are inherent in all algorithms on the IQC as we are presently unable to design pulse sequences for quantum gates without generating unwanted transitions albeit with small probabilities. These errors can in principle be decreased by going sufficiently deep into the selective excitation regime, but one must keep in mind the limitations of real experiments.[b] Coupling with the "environmental" degrees of freedom is endemic in all implementations of quantum computers. As the environment will usually have many degrees of freedom, we shall model its influence on the quantum computer by using some effective perturbation V_{eff} given by a random matrix from a Gaussian unitary ensemble (GUE).[7] Note that the coupling with the environment will generally cause non-unitary evolution of the central system. We expect quantum

[b]A new method for dealing with intrinsic errors has been proposed recently in Ref. 15.

computation to be stable only on a time scale where the evolution of the quantum computer is approximately unitary, i.e. for times smaller than the non-unitarity time scale. Therefore, we limit ourselves to *unitary* external perturbations. The third kind of errors due to the variation of system parameters, e.g. variation of Larmor frequencies due to changes of the magnetic field are not considered in this paper. This does not mean they are not important. Let us consider a systematic error in the gradient of the magnetic field throughout the protocol ($a \to a + \delta a$). Demanding that the error in the largest eigenphase at the end of the algorithm is much smaller than 1, one gets the condition $a/\delta a \approx an^{p+2}/\Omega$. If one is in the selective excitation regime, this ratio can become very large and this puts stringent demands on experiment.

To ease understanding, we shall first discuss intrinsic errors only, then external ones and finally both combined.

4.1. *Intrinsic errors*

For near-resonant and non-resonant transitions we have $\Delta \gg \Omega$ and the probability given by perturbation theory is $p \propto (\Omega/\Delta)^2$. In the $2\pi k$ method, the Rabi frequency Ω is approximately J/k [see Eq. (4)] so the probabilities for near-resonant ($\Delta \sim J$) and non-resonant ($\Delta \sim a$) transitions are

$$\begin{aligned} p^{\text{near}} &\propto \left(\frac{1}{k}\right)^2 \\ p_{jl}^{\text{non}} &\propto \left(\frac{J}{ka(j-l)}\right)^2, \end{aligned} \tag{13}$$

respectively. p_{jl}^{non} denotes the probability of a non-resonant transition with $\Delta \approx a|j-l|$ involving the jth spin (resonant with the transition) and the lth spin (erroneously flipped due to the unwanted transition). The dependence of near and non-resonant errors on system parameters is therefore different.

In pulse sequences implementing the QFT or the IQFT, we always use the generalized $2\pi k$ method by which one can get rid of all near-resonant transitions. Therefore, the only errors that remain are non-resonant ones. We first checked numerically that this is indeed the case by studying dependence of errors on system parameters by which one is able to distinguish near and non-resonant errors, Eq. (13).

One can observe from Fig. 1 that agreement with the theoretical p^{non} [Eq. (13)] is excellent thereby confirming that the only errors left are the non-resonant ones. By using the generalized $2\pi k$ method, we decreased intrinsic errors by a factor of $(a/J)^2$ as compared to the ordinary $2\pi k$ method, where there are still some near-resonant errors present. In order to have a complete understanding of fidelity decay due to intrinsic errors, we have to understand scaling of these with the number of qubits. As we already discussed in Sec. 3, this depends on two things: how strong the errors are correlated, giving possible scalings from n^p to n^{2p} and on the

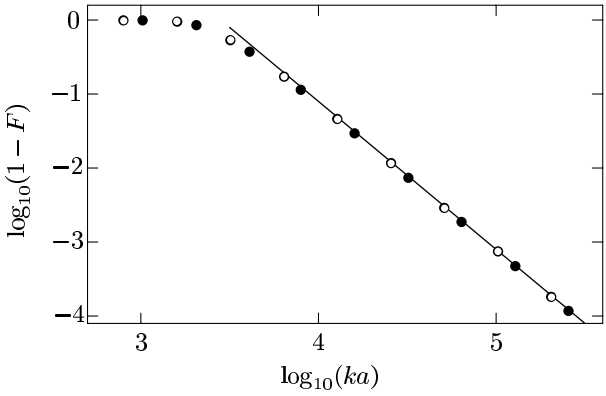

Fig. 1. Dependence of fidelity for the QFT on physical parameters of the system. Empty points indicate variation of k with $a = 100$ and filled points indicate variation of a with $k = 128$, both for $n = 6$. The full line is the theoretical dependence of p^{non} on system parameters given by Eq. (13). The agreement with the theoretical dependence confirms that the only errors left are non-resonant ones.

dependence of the perturbation strength with the number of qubits. Let us first discuss the latter.

Under the assumption that the average transition probability (i.e. perturbation strength) for a non-resonant transition is the sum of all possible non-resonant transitions averaged over all possible resonant qubits, we can estimate

$$\delta^2 \propto \frac{1}{n} \sum_{j \neq l=0}^{n-1} p_{jl}^{\text{non}} \xrightarrow{n\to\infty} \left[\frac{J}{ka}\right]^2 \left(\frac{\pi^2}{3} - \alpha \frac{\log n}{n}\right), \tag{14}$$

with α some n independent constant. We can see that the perturbation strength approaches a fixed value as n grows, but the convergence to its limit is logarithmically slow. For small n, the perturbation strength therefore will grow with n, whereas it will saturate for large n.

The second contribution to the n-dependence of fidelity comes from the dynamical correlations between errors given by the correlation function (12) of the perturbation generator for non-resonant errors. We numerically calculated this correlation function in order to understand how the correlation sum, and therefore fidelity behaves as a function of n.

In Fig. 2, we show $C(t_1, t_2)$ averaged over all Hilbert space. One can see that there are large two-dimensional regions of high correlations in all parts of the picture. Thus, there are strong correlations between errors at different pulses and the correlation sum will grow as $\sim n^6$ as the number of pulses scales as n^3 for our implementation of the QFT. Similar results are also obtained for the IQFT as can be inferred from Fig. 4. Note that during the application of the transposition gate at the end of the protocol, the correlation sum starts to decrease, nicely seen in Fig. 3 and also visible in the correlation picture in Fig. 2 as there are more negative than positive areas towards the end of the algorithm. This very interesting

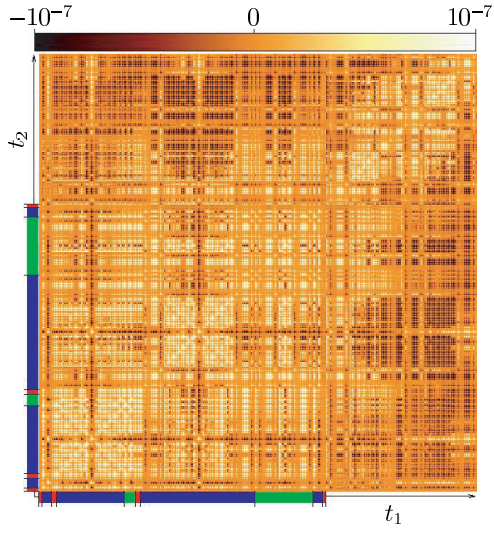

Fig. 2. Correlation function for intrinsic errors in the QFT for $k = 128$, $a = 100$ and $n = 4$. The shading on the time axes denotes the duration of different gates, Eq. (5), and the time going from 1 to 543 runs over all Q-pulses. The light/dark areas give a positive/negative contribution to the fidelity.

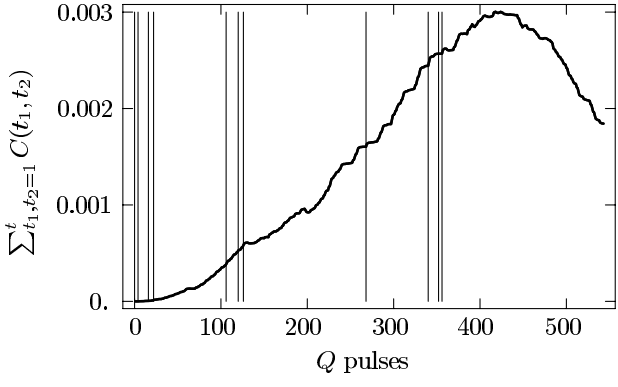

Fig. 3. The correlation sum of the same data as in Fig. 2. Note the decrease of the sum when the transposition gate is applied. The fidelity is in this linear response regime simply given by Eq. (11). Vertical lines indicate the beginning of each gate [Eq. (5)].

phenomenon means that applying the transposition gate is advantageous as it will increase fidelity. Note that this would not occur if we would do the transposition operation digitally after the readout. We checked that this principle cannot be exploited further by repeating the transposition many times and by this decreasing correlation sum even more. Still, this surprising behavior suggests that it might be possible to decrease non-resonant errors in a systematic way.

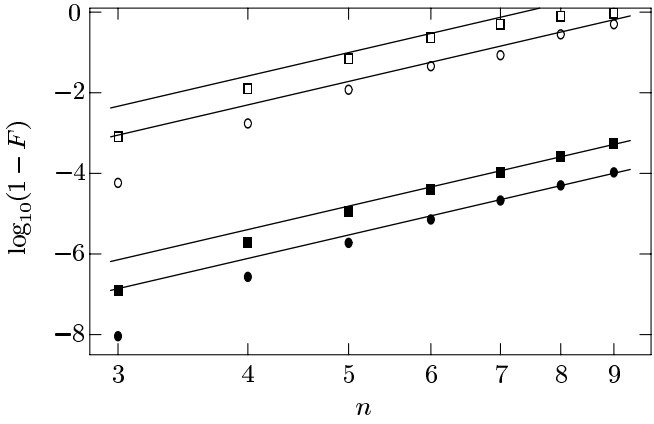

Fig. 4. Dependence of fidelity on the number of qubits. Empty symbols indicate data for $k = 128$ and $a = 100$ while filled symbols are for $k = 1{,}024$ and $a = 1{,}000$. Circles indicate the QFT and squares the IQFT. In the presence of intrinsic errors *only*, the IQFT does not improve fidelity. Full lines show the asymptotic n^6 dependence.

To further confirm the predicted $\sim n^6$ growth of the correlation sum, we calculated the dependence of intrinsic errors on n. This can be seen in Fig. 4, where we plot $1 - F(T)$ as a function of n for the QFT and the IQFT, for two different sets of parameters, one for $k = 128$, $a = 100$ giving large errors and one for $k = 1{,}024$, $a = 1{,}000$. One can see that asymptotically for large n the dependence is indeed n^6, but one needs of the order of $n = 7$ or more qubits for convergence. This slow convergence we believe is due to the logarithmic convergence of the perturbation strength [Eq. (14)]. To get exact coefficients in front of the n^6 dependence term, we fitted dependences of errors in Fig. 4 with a polynomial in n using at most two nonzero terms. Defining polynomials in the linear response regime as $s^{\text{in}} = (1 - F)(ka/J)^2$, one gets for the QFT and the IQFT:

$$\begin{aligned} s^{\text{in}}_{\text{QFT}}(n) &= 280n^6 - 660n^5 \\ s^{\text{in}}_{\text{IQFT}}(n) &= 1300n^6 - 2100n^5. \end{aligned} \tag{15}$$

Both expressions are good for $n \geq 5$ and superscript "in" denotes intrinsic errors. Beyond the linear response, the exponential dependence is frequently justified[9] and one has

$$F = \exp\left(- \left[\frac{J}{ka} \right]^2 s^{\text{in}}(n) \right). \tag{16}$$

The large coefficients of the polynomials in Eqs. (15) are due to the large number of pulses. The maximum possible dependence in the case of no decay of the correlation function (see discussion at the end of Sec. 3) could be T^2 and therefore the leading terms in the polynomials (15) expressed in terms of the total number of pulses are $s^{\text{in}}_{\text{QFT}} \sim 0.8T^2_{\text{QFT}}$ and $s^{\text{in}}_{\text{IQFT}} \sim 0.5T^2_{\text{IQFT}}$. Therefore, relative to the number of pulses the IQFT slightly decreases non-resonant errors but in the absolute sense the QFT

is better simply because it has only one third as many pulses as the IQFT and the coefficient in front of n^6 [Eq. (15)] is thereby smaller. If only intrinsic errors in the generalized $2\pi k$ method are concerned, the QFT is always more stable than the IQFT. Note that the intrinsic errors due to non-resonant transitions for the QFT grow as $\sim T^2$ ($\sim n^6$) whereas in previously studied "simple" algorithms, such as the entanglement protocol,[4] they grow only as the first power of the number of gates $\sim T$. This means that the QFT is much more sensitive to intrinsic errors.

4.2. *External errors*

In order to study external errors only, we set throughout this section $k = 1{,}024$ and $a = 1{,}000$, for which the intrinsic errors are much smaller than external ones in the range of qubits and perturbation strength considered.

External errors will be modeled with the perturbation V [Eq. (10)] chosen to be a random Hermitian matrix from a GUE ensemble. To facilitate comparison with previous results on the IQFT,[8] we shall apply the perturbation after each quantum gate, except for the last transposition gate T after which we do not apply the perturbation. So for the QFT, we apply $n(n+1)/2$ perturbations, while for the IQFT, we apply n^2 perturbations. Another possible choice would be to apply the perturbations after each pulse. We shall discuss this possibility at the end of this section. For now, let us just say that qualitatively the results are the same as if doing the perturbation after each gate — one just has to rescale the perturbation strength like $\delta_{\text{gate}} \propto n\delta_{\text{pulse}}$ as there are effectively $\mathcal{O}(n)$ perturbations (pulses) per gate.

From the linear response expression for fidelity, we argued that the static perturbations are the worst ones. Hence, we will consider only static perturbations, i.e. the same perturbation for all gates. As the QFT is implemented in the interaction picture, one expects that the worst perturbation has to be static in the interaction picture and not in the Schrödinger one. Remember that the transformation between the interaction and the Schrödinger picture is given by a unitary transformation $W(t) = \exp(-\mathrm{i}H_0 t)$ generated by the time independent part of the whole Hamiltonian H in Eq. (1), $\psi_{\text{int}}(t) = W^\dagger(t)\psi_{\text{sch}}(t)$. To verify this, we compared the error growth for a static perturbation applied in the interaction picture (i.e. the wave function after one application of error is $\psi^\delta_{\text{int}} = \exp(-\mathrm{i}\delta V)\psi_{\text{int}}$) with the errors for a static perturbation in the Schrödinger picture ($\psi^\delta_{\text{sch}} = \exp(-\mathrm{i}\delta V)\psi_{\text{sch}}$). Let us first consider the latter.

If we apply a static perturbation in the Schrödinger picture, we can transform it to the interaction picture by $W(t)$. This transformation, using

$$\exp(-\mathrm{i}\delta V_{\text{int}}(t)) := W^\dagger(t)\exp(-\mathrm{i}\delta V_{\text{sch}})W(t), \tag{17}$$

will result in the perturbation in the interaction picture $V_{\text{int}}(t)$ being time dependent. As this transformation involves large phases in the selective excitation regime, perturbations at different gates will tend to be uncorrelated due to averaging

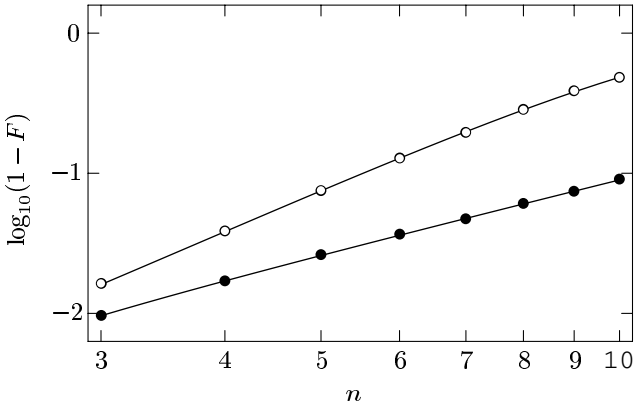

Fig. 5. Dependence of $1 - F$ in the QFT algorithm on the number of qubits for static perturbation in the interaction picture (empty points) and in the Schrödinger picture (full points), with $\delta = 0.04$. Lines are the best fitting polynomials [see Eq. (18)]. We can see that static perturbations in the interaction picture are more damaging than static perturbations in the Schrödinger picture.

of widely oscillating factors in the correlation function (12). Therefore, to first approximation one can assume $C(t_1, t_2) = \delta_{t_1,t_2}$ so the fidelity will decay as $F(T) = \exp(-\delta^2 T)$.[8] On the other hand, if we select the perturbation to be static in the interaction picture the correlation function will not be a Kronecker delta in time, so the fidelity will decay faster.

To numerically confirm these arguments, we show in Fig. 5, the dependence of fidelity on the number of qubits n for the two cases discussed: static perturbation in the interaction picture and static perturbation in the Schrödinger picture. Polynomial fitting of the n dependence for the QFT gives

$$\begin{aligned} s_{\text{sch}}^{\text{gue}}(n) &= 0.47n^2 + 1.41n - 2.42, \\ s_{\text{int}}^{\text{gue}}(n) &= 0.45n^3 - 0.42n^2 + 0.58n. \end{aligned} \tag{18}$$

The fidelity due to external GUE errors is then given as

$$F = \exp(-\delta^2 s^{\text{gue}}(n)), \tag{19}$$

with the appropriate $s^{\text{gue}}(n)$ from Eq. (18). Note that $s_{\text{int}}^{\text{gue}}(n)$ grows faster than $s_{\text{sch}}^{\text{gue}}(n)$, thereby confirming our expectations. Observe also that for static perturbations in the Schrödinger picture, using the assumption of completely uncorrelated errors in the interaction picture, we predicted $s_{\text{sch}}^{\text{gue}} \approx T \approx n^2/2$ for the QFT, which is remarkably close to the numerically observed value $0.47n^2$ in Eq. (18). For the IQFT and the application of GUE perturbation in the Schrödinger picture, one gets a similar result with the leading term $s_{\text{sch}}^{\text{gue}}(n) \sim 1.12n^2$. One can write an arbitrary time dependent perturbation in the interaction picture as a Fourier series and for large n the static component will always prevail. Therefore, from now on we shall exclusively discuss only static perturbations in the interaction picture.

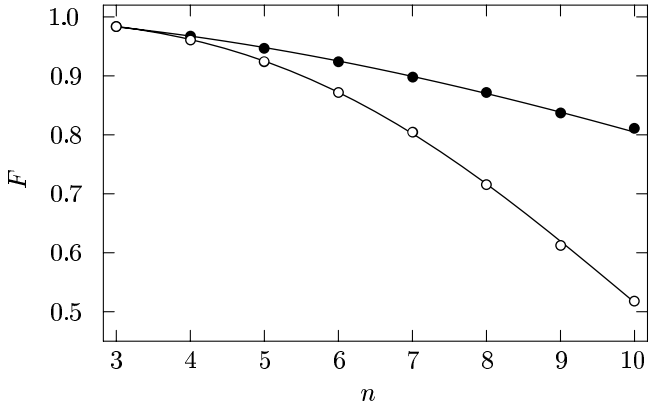

Fig. 6. Dependence of the fidelity on the number of qubits for the QFT (empty symbols) and the IQFT (filled symbols) algorithms ($\delta = 0.04$). Curves indicate the theoretical prediction Eq. (19) using the polynomials from Eqs. (20) and (18).

The dependence of errors due to GUE perturbations in the case of the QFT and the IQFT has already been derived.[c] For the IQFT numerical fitting in our case gives dependence

$$s^{\mathrm{gue}}_{\mathrm{IQFT}}(n) = 1.31n^2 + 0.86n - 3.73. \tag{20}$$

Dependence of fidelity in both cases can be seen in Fig. 6, together with the theoretical prediction [Eq. (19)] using the polynomials (18) and (20).

Observe that the IQFT for $n > n_{\mathrm{crit}} = 3$ is better than the QFT despite having more gates and therefore applying the perturbation on it more times (for $n = 3$ the QFT is slightly better). What is important is that the dependence of errors on n is also different: $\sim n^3$ for the QFT, but only $\sim n^2$ for the IQFT. This means that asymptotically the IQFT is much more stable against GUE perturbations than the ordinary QFT.

Finally, let us discuss what happens if we apply static GUE perturbations after *each pulse*, instead of after each gate as done so far.

Let U_j denote a single pulse, $(U_r \cdots U_1)$ the whole gate and $V(j) = (U_j \cdots U_1)^\dagger V (U_j \cdots U_1)$. To the lowest order in δ, we can rewrite the perturbed gate as

$$\exp(-\mathrm{i}\delta V) U_r \cdots \exp(-\mathrm{i}\delta V) U_1 \approx U_r \cdots U_1 \exp\left(-\mathrm{i}\delta [V(1) + \cdots + V(r)]\right), \tag{21}$$

where we moved all the perturbations to the beginning of the gate. This means that the application of the perturbation after each pulse is to the lowest order in δ *equivalent* to the application of the effective perturbation $\delta \sum_j^r V(j)$ after the gate. Of course now the perturbation is explicitly time dependent. But individual pulses

[c] Taking into account the different definition of fidelity in Ref. 8, polynomials are almost the same with the slight difference due to the different number of applied perturbations.

will do transformations on an exponentially small subspace of the GUE matrix (i.e. on one qubit) and therefore one might expect that effectively $\sum_j^r V(j) \approx rV_{\text{eff}}$, where V_{eff} is some effective random matrix independent of the gate and very similar to V. As in our case of the QFT, on the IQC we have on average $\propto n$ pulses per gate, we can predict that applying a perturbation with strength δ_{pulse} after each pulse is approximately equal to applying a perturbation of strength $\delta_{\text{gate}} \approx n\delta_{\text{pulse}}$ after each gate. In order to confirm these expectations, we did numerical experiments with the results shown in Fig. 7. Fitting a polynomial in the dependence of fidelity, Eq. (19), for the QFT and the IQFT gives in this case

$$\begin{aligned} s_{\text{QFT}}^{\text{gue}}(n) &= 4.86n^5 + 35.8n^4, \\ s_{\text{IQFT}}^{\text{gue}}(n) &= 25.6n^4 + 606n^3. \end{aligned} \tag{22}$$

The leading dependence of n^5 for the QFT and n^4 for the IQFT agrees nicely with our rescaling prediction $\delta_{\text{gate}} \approx n\delta_{\text{pulse}}$. The IQFT is asymptotically again better than the QFT as the errors grow slower with the number of qubits. The crossing point between the two in this case happens at $n_{\text{crit}} = 10$, whereas in the case of perturbation after each gate we had $n_{\text{crit}} = 3$. This confirms that doing GUE perturbation after each pulse is qualitatively the same as doing it after each gate: only the crossing point between the QFT and the IQFT is shifted. The dependence of errors on n changes simply due to the different number of applied perturbations. If the perturbation strength δ is properly rescaled, the n dependence is the same in both cases.

Up to now, we have discussed intrinsic errors and external errors separately. The next question is of course, what happens if both errors are present at the same time and are of similar strength?

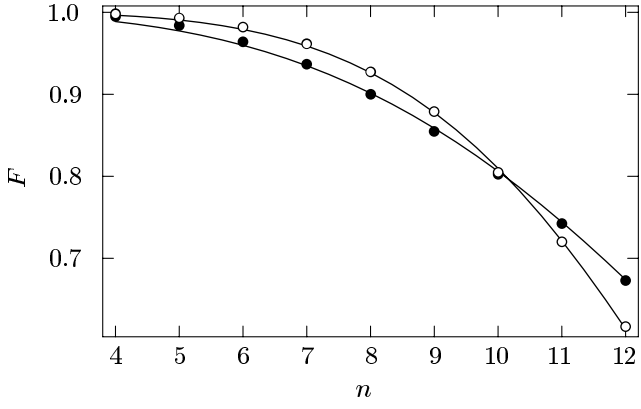

Fig. 7. Dependence of F on the number of qubits for the static GUE perturbation after each pulse with $\delta = 5 \times 10^{-4}$. Empty symbols are for the QFT and filled symbols are for the IQFT. For large n, the IQFT is again better than the QFT. Curves are the theoretical prediction Eq. (19) using the best fitting polynomials given by Eq. (22).

4.3. *Intrinsic and external errors combined*

If both kinds of errors are present, a first naive guess would be that they just add,

$$F^{\text{both}} \approx F^{\text{in}} F^{\text{gue}} = \exp\left(-\left[\frac{J}{ka}\right]^2 s^{\text{in}}(n) - \delta^2 s^{\text{gue}}(n) \right), \tag{23}$$

with the appropriate polynomials $s^{\text{in}}(n)$ and $s^{\text{gue}}(n)$ given in Eqs. (15), (18) and (20). In the linear response regime, this formula means that both errors are uncorrelated, i.e. their cross-correlations are zero. This is easy to prove using properties of GUE matrices. Let us calculate the cross-correlation function between intrinsic perturbation, $V^{\text{in}}(t_1)$, and external perturbation, $V^{\text{gue}}(t_2)$, averaged over the GUE ensemble. Written explicitly, one has to average products of the form $V^{\text{in}}_{ij} V^{\text{gue}}_{jk}$. As this expression is linear in V^{gue}, it averages to zero, $\langle V^{\text{in}}_{ij} V^{\text{gue}}_{jk} \rangle_{\text{gue}} = 0$, thereby explicitly confirming a simple addition of both errors. Of course in real experiments, we are not averaging over a GUE ensemble but we are taking one definite representative member of it. For large Hilbert space, the expectation value of a typical random state and one particular GUE matrix is "self-averaging" and will be equal to the ensemble average.

Let us check the theoretical prediction for fidelity Eq. (23) with a numerical experiment. The results together with the theoretical prediction Eq. (23) are in Fig. 8. The agreement between theory and experiment is good even beyond the linear response regime. Please note that we deliberately choose parameters such that both the QFT and the IQFT give similar fidelity in order to also see the crossing of the two curves within the shown range of n. Given a fixed δ and ka, the QFT is always better for large n because intrinsic errors will prevail over external

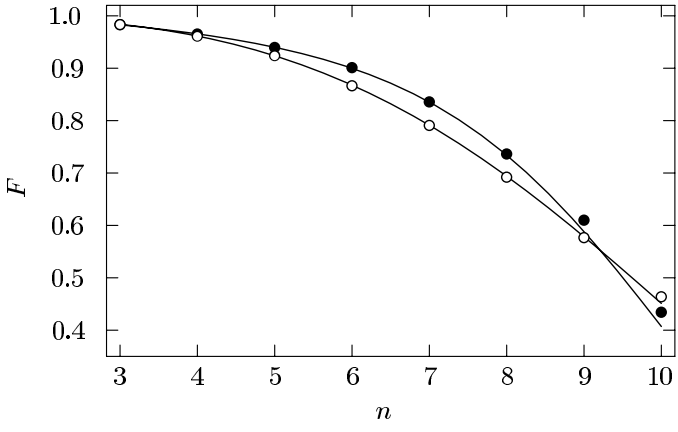

Fig. 8. Fidelity for the QFT (empty symbols) and the IQFT (filled symbols) algorithm with GUE perturbation after each gate. System parameters are $k = a = 200$ and $\delta = 0.04$ (intrinsic and external errors are comparable in size). Full curves are theoretical predictions for F given by Eq. (23). With both errors present, the QFT is always better than the IQFT for large enough n.

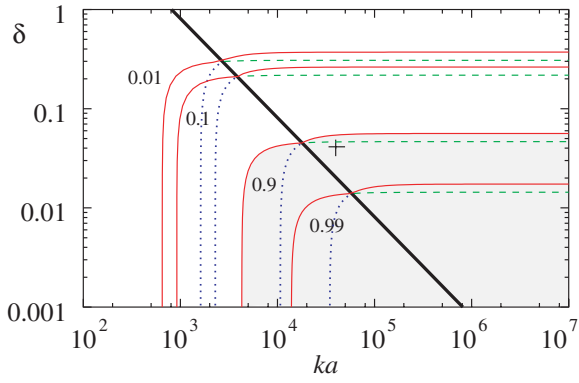

Fig. 9. The dependence of fidelity on system parameter ka and GUE perturbation strength δ for $n = 5$. Full curves of constant fidelity are composed of two parts corresponding to the QFT or the IQFT. To the right of the thick line for δ_{crit}, the IQFT is better and below the QFT is better. Dotted curves of constant fidelity below this line are for the IQFT and dashed lines above are for the QFT. The shaded region corresponds to the region of fidelity larger than 0.9. The plus symbol shows the position of parameters for Fig. 8.

ones, due to their fast n^6 growth. But still, for intermediate n's, the IQFT can be better than the QFT as seen in Fig. 8.

Equipped with the understanding of errors in the QFT and the IQFT due to external GUE perturbations and intrinsic errors, we can make some predictions regarding ranges of experimental parameters ka, δ, n for which the fidelity will be high enough. An interesting question is, when is the IQFT better than the QFT? Setting $F_{\text{QFT}} = F_{\text{IQFT}}$ with F's given by Eq. (23) results in the condition

$$\delta_{\text{crit}} = \frac{J}{ka}\sqrt{\frac{s^{\text{in}}_{\text{QFT}} - s^{\text{in}}_{\text{IQFT}}}{s^{\text{gue}}_{\text{QFT}} - s^{\text{gue}}_{\text{IQFT}}}}. \tag{24}$$

For $\delta > \delta_{\text{crit}}$, the IQFT is better than the QFT. In Fig. 9, we show curves of constant fidelity for $n = 5$. They are composed of two parts. To the right of the line for δ_{crit}, the IQFT is better than the QFT, and *vice versa*. Two characteristic features are also vertical and horizontal asymptotes of curves of constant fidelity. Vertical asymptotes mean that for a fixed n, even if $\delta = 0$, we must have ka larger than some critical value determined just by intrinsic errors, in order to have a given fidelity. Horizontal asymptotes for high ka mean that if δ is larger than some critical value, increasing ka will not help to improve fidelity. In Figs. 10 and 11, we show similar plots, only now one of the axes gives the dependence on n. For instance, from Fig. 10 on can see that fixing $ka = 10^5$, the maximum number of qubits is $n \approx 12$ if we want to have fidelity larger than 0.9 (even if $\delta = 0$). This unfavorable growth of required $ka \propto n^3$ in order to have a fixed fidelity is due to the $\sim n^6$ growth of intrinsic errors. It would therefore be advantageous to find a way to suppress errors due to non-resonant transitions.[16]

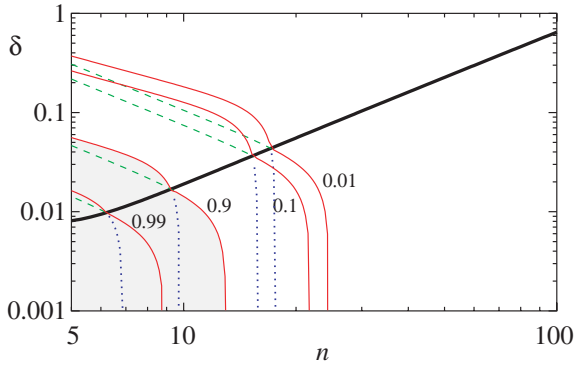

Fig. 10. Fidelity dependence on δ and number of qubits n for $ka = 10^5$. IQFT is better above the thick line. For the explanation of the curves, see the caption of Fig. 9.

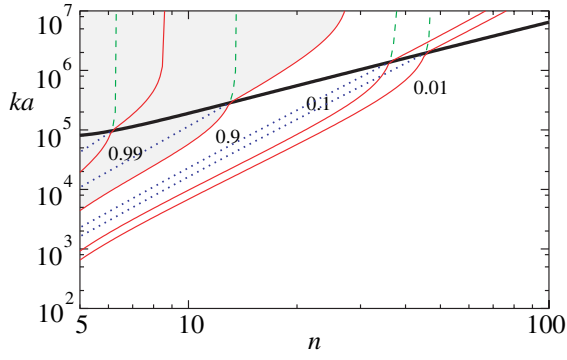

Fig. 11. Fidelity dependence on ka and n for $\delta = 0.01$. IQFT is better above the thick line. For the explanation of the curves see the caption of Fig. 9.

5. Conclusions

We have analyzed two possible errors in the implementation of an algorithm on a quantum computer. In particular, we discuss the implementation of the QFT on the IQC. We consider: (i) intrinsic errors due to unwanted transitions caused by pulses, and (ii) external errors due to the coupling with the external degrees of freedom. We carefully analyze their dependence on system parameters, particularly on the number of qubits. To diminish intrinsic errors, we use the generalized $2\pi k$ method by which we are able to suppress all near-resonant transitions, with only much smaller non-resonant transitions remaining. We then study these non-resonant errors in the QFT algorithm and by using a correlation function formalism explain their growth with time as $\sim T^2$, in contrast to existing "simple" algorithms (having $\mathcal{O}(n)$ gates), where the growth is linear in time. This very fast growth with n is a consequence of strong correlations between non-resonant errors at different pulses. In view of this, it would certainly be desirable to find a way to suppress non-resonant errors, e.g. to uncorrelate or anti-correlate them.

Two interesting questions immediately impose themselves: Is this behavior general also for other models of quantum computers where the pulses (gates) are not perfect and whether this fast growth of errors is general for all algorithms having more than $\mathcal{O}(n)$ gates? This is very important as the $\sim T^2$ growth would mean that the problem of actually building a large quantum computer executing a complex algorithm is much harder than previously thought, since the correlations of errors at different time steps can significantly influence the stability.

We also consider perturbations due to the coupling with the external degrees of freedom modeled by a random GUE matrix. To suppress this kind of error, we show that it is advantageous to use an improved QFT algorithm, even in the presence of intrinsic errors. For the IQFT, these external errors grow only as $\sim n^2$, whereas they grow as $\sim n^3$ for an ordinary QFT. The improvement of quantum Fourier transformation by using an IQFT algorithm is independent of the specific model used for the quantum computer as it depends only on the sequence of gates (algorithm) and on the external perturbation being a random GUE matrix. This result is particularly appealing as some argue that the external influences will be the main limiting factor in the construction of quantum computers and therefore using the IQFT can significantly improve performance in the limit of a large number of qubits.

Acknowledgments

Useful discussions with T. Prosen, T. H. Seligman, G. P. Berman, F. Borgonovi and R. Bonifacio, are gratefully acknowledged. The work of C.P. was supported by Dirección General de Estudios de Posgrado (DGEP) and CONACYT grant 41000-F. C.P. is grateful to the University of Ljubljana and the Universita Cattolica at Brescia for hospitality. The work of M. Ž. has been financially supported by the Ministry of Science, Education and Sport of Slovenia.

Appendix. QFT and IQFT Implementation on the Ising Quantum Computer

To implement the protocol with high fidelity, we use $Q_{i\rho}^{ab}$ pulses derived in Ref. 6, which completely suppress all near-resonant errors. Phases of Q-pulses composing a gate must be chosen such that the gate works on an arbitrary state. The protocols implementing CN_{ij} (control not gate) and N_j (not gate) can be found in Secs. 7.1–7.3 of Ref. 6.

In order to complete the QFT and the IQFT, we still need to implement the $\mathrm{R}^\dagger$, R, A, B and T gates. We can decompose R, $\mathrm{R}^\dagger$ and T gates into simpler pieces:

$$\mathrm{R}_{ij} = \mathrm{N}_i \mathrm{CN}_{ij} \mathrm{N}_i \mathrm{Z}_j, \tag{A.1}$$

$$\mathrm{R}_{ij}^\dagger = \mathrm{N}_i \mathrm{Z}_j \mathrm{CN}_{ij} \mathrm{N}_i, \tag{A.2}$$

$$\mathrm{T} = \prod_{i=1}^{q} \prod_{j=1}^{q-i} \mathrm{S}_{q-j,q-j-1} \tag{A.3}$$

with $\mathrm{S}_{ij} = \mathrm{CN}_{ij}\mathrm{CN}_{ji}\mathrm{CN}_{ij}$ the swap gate, $\mathrm{Z} = \mathrm{diag}\{1, -1\}$ the σ_z gate, and each term in the product in Eq. (A.3) is placed on the left of the sub-product (e.g. $\prod_{i=0}^{2} D_i = D_2 D_1 D_0$). Therefore, the only gates left to design are A, B and Z.

The phases of Q-pulses can be expressed in terms of angles θ_ρ, α_ρ, Θ_ρ, β_ρ and γ_ρ,[6] which are given by

$$\theta_\rho = \pi\sqrt{k_\rho^2 - \rho^2/4}, \tag{A.4}$$

$$\alpha_\rho = \frac{\pi}{2}\sqrt{k_\rho^2 + 3\rho^2/4}, \tag{A.5}$$

$$\tan\Theta_\rho = -\frac{\theta_\rho}{2\alpha_\rho}\tan\alpha_\rho, \tag{A.6}$$

$$\tan\beta_\rho = -\frac{\pi}{2\alpha_\rho}\tan\alpha_\rho\cos\Theta_\rho, \tag{A.7}$$

$$\gamma_\rho = \sqrt{(\pi k_\rho)^2 - (\pi + \beta_\rho)^2}. \tag{A.8}$$

We use notation of angles without subscripts denoting angles for π pulses, i.e. $\theta \equiv \theta_1$ and set $k_{1/2} = 2k$.

The Hadamard gate can now be expressed as

$$\mathrm{A}_j = Q_j^{00}(\varphi_1)Q_j^{10}(\varphi_2)Q_j^{11}(\varphi_3)Q_{j\frac{1}{2}}^{00}(\varphi_4)Q_{j\frac{1}{2}}^{10}(\varphi_5)Q_{j\frac{1}{2}}^{11}(\pi/2), \tag{A.9}$$

for intermediate qubits and

$$\mathrm{A}_j = Q_j^{0}(\varphi_6)Q_j^{1}(\varphi_7)Q_{j\frac{1}{2}}^{0}(\varphi_8)Q_{j\frac{1}{2}}^{1}(\pi/2), \tag{A.10}$$

for edge qubits, with

$$\begin{aligned}
&\varphi_1 = -2\big(\theta + \gamma_{\frac{1}{2}} + \theta_{\frac{1}{2}}\big), && \varphi_2 = -\theta - 2\Theta,\\
&\varphi_3 = -2\big(\theta + \gamma - \gamma_{\frac{1}{2}} - \theta_{\frac{1}{2}}\big), && \varphi_4 = \pi/2 - 2\gamma - 4\theta_{\frac{1}{2}},\\
&\varphi_5 = \pi/2 - \theta_{\frac{1}{2}} - 2\Theta_{\frac{1}{2}}, && \varphi_6 = -\theta - \theta_{\frac{1}{2}},\\
&\varphi_7 = -\theta + \theta_{\frac{1}{2}}, && \varphi_8 = \pi/2 - 2\theta_{\frac{1}{2}}.
\end{aligned} \tag{A.11}$$

For neighboring qubits ($|i - j| = 1$), the B gate can be written as

$$\begin{aligned}
\mathrm{B}_{ij} = {} & Q_i^{11}(0)Q_i^{10}(0)Q_i^{00}(0)Q_j^{10}(0)Q_j^{10}(\varphi_1)Q_j^{00}(0)\\
& \times Q_j^{00}(\varphi_2)Q_i^{11}(\varphi_3)Q_i^{10}(\varphi_3)Q_i^{00}(\varphi_3)Q_j^{10}(0)\\
& \times Q_j^{10}(\varphi_4)Q_j^{11}(0)Q_j^{11}(\varphi_5),
\end{aligned} \tag{A.12}$$

for intermediate qubits and for edge qubits (i or $j \in \{0, n-1\}$) it is

$$\begin{aligned}
\mathrm{B}_{ij} = {} & Q_i^{1}(0)Q_i^{0}(0)Q_j^{10}(0)Q_j^{10}(0)Q_j^{00}(0)\\
& \times Q_j^{00}(\varphi_6)Q_i^{1}(\varphi_7)Q_i^{0}(\varphi_8)Q_j^{10}(0)\\
& \times Q_j^{10}(\varphi_9)Q_j^{11}(0)Q_j^{11}(\varphi_{10}).
\end{aligned} \tag{A.13}$$

Angles for B gates are

$$\begin{aligned}
\varphi_1 &= -2\gamma - 3\theta + 2\Theta, & \varphi_2 &= \phi/2 - 2\gamma - 6\theta, \\
\varphi_3 &= \phi/4 - \pi/2, & \varphi_4 &= -\varphi_1, \\
\varphi_5 &= \phi/2 + 2\gamma + 6\theta, & \varphi_6 &= \phi/2 - 6\gamma - 12\theta + 4\Theta, \\
\varphi_7 &= \varphi_3 - \varphi_1, & \varphi_8 &= \varphi_3 + \varphi_1, \\
\varphi_9 &= -2\varphi_1, & \varphi_{10} &= \phi/2 - 2\gamma + 4\Theta,
\end{aligned} \tag{A.14}$$

and $\phi = \pi/2$. For distant qubits ($|i - j| > 1$), it is necessary to use swap gates to bring ith and jth qubits to neighboring positions, then apply B protocol for neighbor qubits and finally take them back to their original positions using swap gates. The angle ϕ in Eq. (A.14) is in this case $\phi = \pi/2^{|j-i|}$. Finally, the Z gate is expressed as

$$\mathrm{Z}_j = Q_j^{11}(0)Q_j^{10}(0)Q_j^{00}(0)Q_j^{11}(\pi/2)Q_j^{10}(\pi/2)Q_j^{00}(\pi/2) \tag{A.15}$$

for intermediate qubits and

$$\mathrm{Z}_j = Q_j^{1}(0)Q_j^{0}(0)Q_j^{1}(\pi/2)Q_j^{0}(\pi/2) \tag{A.16}$$

for edge qubits. Counting the number of all pulses for QFT and IQFT, one gets

$$T_{\mathrm{QFT}} = 18n^3 - 16n^2 - 49n + 57, \tag{A.17}$$

$$T_{\mathrm{IQFT}} = 54n^3 - 86n^2 - 105n + 191. \tag{A.18}$$

References

1. C. H. Bennett and D. P. DiVincenzo, *Nature* **404**, 247 (2000).
2. G. P. Berman, G. D. Doolen, G. D. Holm and V. I. Tsifrinovich, *Phys. Lett.* **A193**, 444 (1994).
3. P. Shor, in *Procs. 35th Annual Symp. Foundation of Computer Science* (IEEE Computer Society Press, New York 1994), p. 124.
4. G. P. Berman, F. Borgonovi, G. Celardo, F. M. Izrailev and D. I. Kamenev, *Phys. Rev.* **E66**, 056206 (2002).
5. G. P. Berman, G. D. Doolen, G. V. Lopez and V. I. Tsifrinovich, *Phys. Rev.* **A61**, 042307 (2000).
6. G. P. Berman, D. I. Kamenev, R. B. Kassman, C. Pineda and V. I. Tsifrinovich, *Int. J. Quant. Inform.* **1**, 51 (2003).
7. T. Guhr, A. Müller-Groeling and H. A. Weidenmüller, *Phys. Rep.* **299**, 190 (1998).
8. T. Prosen and M. Žnidarič, *J. Phys. A: Math. Gen.* **34**, L681 (2001).
9. T. Prosen and M. Žnidarič, *J. Phys. A: Math. Gen.* **35**, 1455 (2002); T. Prosen, *Phys. Rev.* **E65**, 036208 (2002).
10. A. M. Steane, in *Decoherence and Its Implications in Quantum Computation and Information Transfer*, eds. C. Vorderman, A. Gonis and P. E. A. Turchi (IOS Press, Amsterdam, 2001), p. 284, also quant-ph/0304016.
11. G. P. Berman, G. D. Doolen, G. V. Lopez and V. I. Tsifrinovich, *Phys. Rev.* **A61**, 062305 (2000).
12. D. G. Cory *et al.*, *Fortschritte der Physik* **48**, 875 (2000).

13. T. Prosen, T. H. Seligman and M. Žnidarič, *Prog. Theo. Phys. Supp.* **150**, 200 (2003).
14. T. Prosen and M. Žnidarič, *New J. Phys.* **5**, 109 (2003).
15. L.-A. Wu and D. A. Lidar, *Phys. Rev. Lett.* **91**, 097904 (2003).
16. G. P. Berman, D. I. Kamenev and V. I. Tsifrinovich, quant-ph/0310049.